Ecosystems (2009) 12: 279–297
DOI: 10.1007/s10021-008-9222-4

ECOSYSTEMS

Estimating Long-Term Changes in China's Village Landscapes

Erle Christopher Ellis,[1]* Nagaraj Neerchal,[2] Kui Peng,[3,4] Hong Sheng Xiao,[5] Hongqing Wang,[1,6] Yan Zhuang,[2] Shou Cheng Li,[7] Jun Xi Wu,[8] Jia Guo Jiao,[9] Hua Ouyang,[3] Xu Cheng,[8] and Lin Zhang Yang[9]

[1]Department of Geography & Environmental Systems, University of Maryland, Baltimore County, 1000 Hilltop Circle, Baltimore, Maryland 21250, USA; [2]Department of Mathematics & Statistics, University of Maryland, Baltimore County, 1000 Hilltop Circle, Baltimore, Maryland 21250, USA; [3]Institute of Geographic Sciences & Natural Resources Research, Chinese Academy of Sciences, Beijing 100101, China; [4]Metallurgical and Ecological Engineering School, University of Science and Technology Beijing, Beijing 100083, China; [5]Institute of Tropical & Subtropical Ecology, South China Agricultural University, Guangzhou, Guangdong 510642, China; [6]Institute of Coastal Ecology and Engineering, University of Louisiana at Lafayette, Lafayette, Louisiana 70504, USA; [7]Agronomy College, Sichuan Agricultural University, Yaan, Sichuan 625014, China; [8]Department of Agronomy & Agroecology, China Agricultural University, Beijing 100094, China; [9]Institute of Soil Science, Chinese Academy of Sciences, Nanjing, Jiangsu 210008, China

Abstract

Over the past 50 years, China's ancient agricultural village landscapes have been transformed by unprecedented social, technological, and ecological changes. Although these dense anthropogenic mosaics of croplands, settlements, and other used lands cover more than 2 million square kilometers across China, the nature of these changes and their environmental impacts remain poorly understood because their spatial scale is generally too small to measure accurately using conventional land-change methods. Here, we investigate the regional consequences of fine-scale landscape changes across China's village regions from 1945 to 2002 using high-resolution, field-validated ecological mapping of a regionally stratified sample of village landscapes at five sites across China, with uncertainties estimated using model-based resampling and Monte Carlo methods. From 1945 to 2002, built surface areas increased by about 7% (90% credible interval = 2–17%) across China's village regions, an increase equivalent to about three times the total urban area of China in 2000. Although this striking result is explained by a near doubling of already large village populations and by lower housing density per capita in rural areas, two unexpected changes were also observed: a 9% net increase (−4% to +21%) in regional cover by closed canopy trees and an 11% net decline (−30% to +3%) in annual crops. These major regional changes were driven primarily by intensive fine-scale land-transformation processes including tree planting and regrowth around new buildings, cropland abandonment, and by the adoption of perennial crops and improved forestry practices. Moreover, the fragmentation, heterogeneity, and complexity of village landscapes increased over time. By coupling regional sampling and upscaling with observations in the field, this study revealed that fine-scale land-change processes in anthropo-

Received 2 June 2008; accepted 12 November 2008;
published online 8 January 2009

Electronic supplementary material: The online version of this article (doi:10.1007/s10021-008-9222-4) contains supplementary material, which is available to authorized users.

E. C. Ellis conceived and managed research, and wrote the article; K. Peng, H. S. Xiao, H. Wang, S. C. Li, J. X. Wu, and J. G. Jiao conducted research; H. Ouyang, X. Cheng, and L. Z. Yang managed research; N. Neerchal and Y. Zhuang contributed methods and models.

*Corresponding author; e-mail: ece@umbc.edu

genic landscapes have the potential for globally significant environmental consequences that are not anticipated, measured, or explained by conventional coarser resolution approaches to global and regional change measurement or modeling.

Key words: human dominated ecosystems; land-use and land-cover change; China; anthropogenic biomes; ecological history; landscape ecology; up-scaling; regional change; ecotope mapping; agriculture.

Introduction

Changes in land use and land cover are a major cause of global changes in biodiversity, biogeochemical cycles, and climate (Vitousek and others 1997; Foley and others 2005; Gibbard and others 2005). Usually considered in terms of deforestation, urban expansion, and other extensive land-transformation processes, the global and regional impacts of intensive fine-scale (<30 m) land transformations are less well understood, even though these tend to be the dominant form of landscape change within densely populated rural, urban, and suburban landscapes (Ellis and others 2006). One reason for this is the challenge in measuring fine-scale landscape changes using the relatively coarse resolution remote sensing platforms that underpin most regional land-change measurements (for example, Landsat, ≥30 m; Ellis and others 2006; Ozdogan and Woodcock 2006). This study will demonstrate that the agricultural village landscapes of China have changed very substantially at fine spatial scales since 1945, with the potential for ecologically significant impacts not only within China but also globally. In so doing, we also demonstrate and assess a new sampling-based methodology for investigating the long-term regional and global changes caused by fine-scale land-transformation processes within densely populated anthropogenic landscapes.

Agricultural village landscapes cover about 8×10^6 km^2 globally, or about 6% of Earth's ice-free land; a global extent several times that of urban landscapes (Ellis and Ramankutty 2008). Occurring predominantly in Asia, these ''village biomes'' are densely populated (≥100 persons km^{-2}) agricultural landscape mosaics that combine croplands with settlements, trees, and a host of other ecologically distinct managed and unmanaged landscape features (Ellis 2004; Ellis and Ramankutty 2008). China's village regions are among the most extensive on Earth, covering about 2×10^6 km^2 across China's eastern plains and central and southern hilly regions (Ellis 2004). Over the past half century, these ancient anthropogenic ecosystems have been transformed by profound social, economic, and technological changes including a near doubling of rural populations, the introduction of industrial inputs for agriculture, and the intensive restructuring of rural landscapes to provide growing populations with improved housing, roads, irrigation, aquaculture, orchards, and rural industry (Han 1989; Heilig 1997; Ellis and others 2000). Although improving rural economic conditions, the ecological impacts of this transition away from traditional village lifestyles and management practices have been severe in many areas, including the pollution of water, soil and air, soil erosion, habitat loss, and the depletion of water and other local resources (Han 1989; Liu and Diamond 2005).

There is no doubt that long-term changes in China's land use and land cover have significantly impacted global biogeochemical cycles and climate (Houghton and Hackler 2003; Zhang and others 2005; Liu and Diamond 2005). However, existing estimates of these impacts are based on coarse-resolution remote sensing, census data, and model-based approximations. Precise estimates of the global contribution of long-term ecological changes within the densely populated village landscapes of China are lacking, even though these landscapes cover approximately 20% of China's total area (Ellis 2004). This is because these studies have focused on recent changes in land cover observable by regional and global remote sensing and on measuring extensive land-change processes such as urbanization, large-scale deforestation, and national afforestation projects (for example, Houghton 2002; Liu and others 2003, 2005a; Seto and Fragkias 2005). As a result, the intensive, fine-scale, landscape-transformation processes that predominate within China's densely populated village regions remain poorly understood (Ellis and others 2000; Ellis 2004).

High-resolution mapping of fine-scale landscape change is too resource-intensive to be practical across large regions and the same is true of field-based ecological measurements and local land management surveys. Yet all of these are necessary to measure and understand the long-term causes and consequences of fine-scale ecological changes within anthropogenic landscapes (Ellis

and others 2000; Grimm and others 2000; Binford and others 2004; Ellis 2004; Rindfuss and others 2004; Wulder and others 2004; Liu and others 2007; Turner and others 2007; Wu and others 2009). Fortunately, stratified sampling techniques can leverage regional data from remote sensing, census statistics, and other extensive data sources to make upscaled regional estimates from relatively small samples of costly fine-scale observations (Gallego and others 1994; Achard and others 2002; Binford and others 2004). Indeed, regional sampling and upscaling has already been used to improve current estimates of China's land use and land cover, and has proved especially effective in its densely populated rural areas where estimates of cropland and other areas have long been suspect (Frolking and others 1999; Zhang and others 2000; Zhao and others 2003).

Unfortunately, sampling long-term ecological changes within China's village landscapes is far more complex. First and foremost, historical landscapes cannot be sampled using spatially random or systematic sampling designs because the spatial extent of historical imagery needed to map them is both nonrandom and spatially restricted (Ellis 2004). Moreover, the costs of field observations in China and other developing rural regions are strongly related to travel distances between samples (Ellis 2004). Given the same resources for fieldwork, this means that random and spatially uniform sampling designs must have smaller sample sizes than spatially clustered designs that restrict sampling to a smaller set of field research sites.

We therefore used a regionally stratified landscape sampling design (Brewer 1999; Schreuder and others 2001) to allocate high-resolution field-validated long-term ecological change measurements to within five 100 km^2 field research sites in environmentally distinct village regions across China (Ellis 2004). We then make regional estimates of long-term landscape changes by coupling measurements from samples with spatially explicit regional datasets for population, land cover, and terrain using two independent regional upscaling and uncertainty analysis procedures. By this approach, we will reveal a variety of ecologically significant and unexpected long-term regional changes within and across the village landscapes of China.

Methods

Regions, Sites, Samples, and Mapping

Regional estimates of long-term changes in China's village landscapes were obtained using a multistage procedure designed to constrain fieldwork, historical and current high-resolution imagery, and other resource-intensive observations within five 100 km^2 field sites across China (Figure 1; Ellis 2004). The methods we used for selecting regions, sites, and samples are detailed in Ellis (2004), preparation of current and historical imagery is described in Wang and Ellis (2005), and our procedures for high-resolution ecological mapping are in Ellis and others (2006). We therefore summarize these methods below and in Figure 1, with

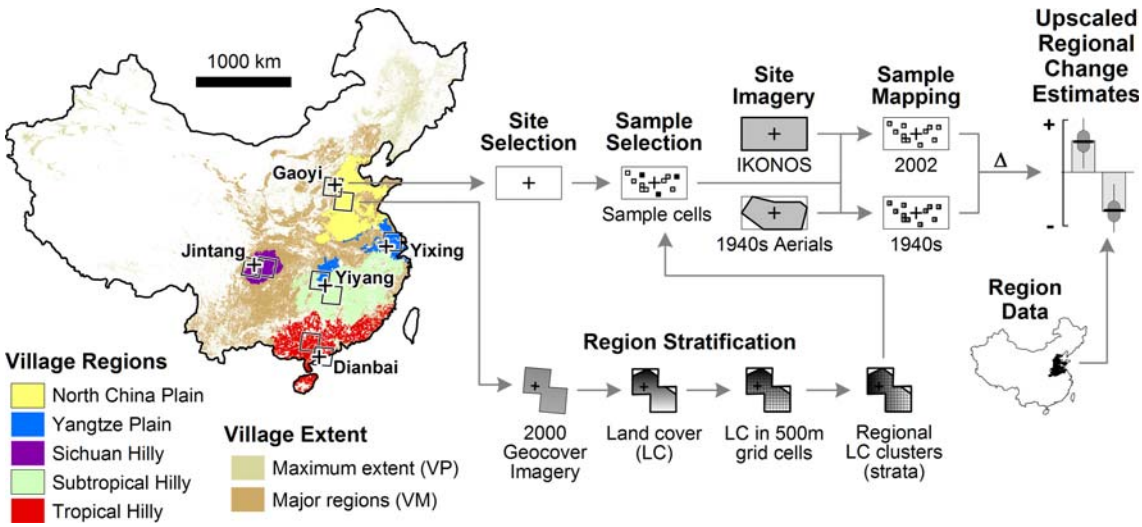

Figure 1. Map of China's village regions and research sites (*left*, site = ''+''; Table 1) and procedures for regional change estimation from site-based landscape samples (*right*; Supplementary material—Appendix 1).

additional details in supplementary material—Appendix 1.

First, China's village regions were stratified into five environmentally distinct regions using a coarse-resolution biophysical cluster analysis (Ellis 2004). A 100 km^2 field site was then selected within each region. Site selection was based on regional data and multiple visits to potential field sites together with regional experts in an extended effort to eliminate any obvious bias in site characteristics relative to village regions as a whole (Ellis 2004). Next, Landsat Geocover 2000 imagery was obtained across a ''subregion'' covering the site within each region, land-cover maps were prepared from these, and then used to estimate percent land cover within 500 × 500 m square grid cells across the subregions (a single grid system was used across China; Ellis 2004). Finally, we identified regional land-cover clusters across the grid cells in each subregion and used these as the basis for selecting a regionally stratified sample of twelve 500 × 500 m grid cells within each site, yielding a total of 60 landscape sample cells across China's village regions (Ellis 2004; Supplementary material—Appendix 1).

High-resolution imagery was acquired across each site in 2002 (IKONOS imagery) and for circa 1945 (archived aerial photographs; Wang and Ellis 2005). Fine-scale ecological maps for 2002 and circa 1945 were made for each landscape sample cell using anthropogenic ecotope mapping, a high-resolution ecological feature mapping procedure based on a combination of high-resolution image interpretation and intensive fieldwork (Figure 2; Ellis and others 2006). This procedure classifies all ecologically distinct features (ecotopes) within landscapes based on a four level *a priori* classification hierarchy, FORM → USE → COVER → GROUP + TYPE, combining basic landform, land-use and land-cover classes (FORM, USE, COVER) with a set of more detailed feature management and vegetation classes (GROUPs) stratified into TYPEs (Ellis and others 2006; http://ecotope.org/aem/classification). Whereas each level of feature classification, including land USE and land COVER, is independent, allowing for separate analysis at each level, full ecotope classification integrates the four classification levels within each feature. For example, a forest of closed canopy regrowth evergreen trees (GROUP + TYPE = en02) on a gentle slope (FORM = SL = Sloping) managed for harvest (USE = T = Forestry) with Perennial COVER (P; >60% woody cover) is classified as the ecotope ''SLTPen02'' (FORM + USE + COVER + GROUP + TYPE).

Region Data

After our landscape samples had been selected and mapped, regional data for land cover, population, and terrain became available across all of China. We therefore made use of these data to improve our mapping of village regions (Figure 1) and to evaluate and strengthen our regional upscaling procedures using complete regional data. Three datasets were obtained: 1 km gridded percent land cover for year 2000 (prepared from 30 m land-cover data: China National Land Cover Dataset; Liu and others 2003), 1 km gridded 2000 population density (Tian and others 2005), and 90 m terrain data (3 arcsecond data from the Shuttle Radar Topography Mission; National Geospatial-Intelligence Agency 2004). These datasets were registered to our original 500 m sample selection grid and interpolated to 500 m using nearest neighbor interpolation (mean in circle with 500 m radius). Mean elevation and percent slope were calculated for 1 km and 500 m grids using GIS (zonal statistics). The 25 land-cover classes were aggregated into 11 simpler classes (Figure 3; including an urban class that was excluded from village regions).

The maximum potential extent of village landscapes in China (VP; Table 1, Figure 1) was mapped at 1 km resolution by selecting the extent of 1 km cells with population between 100 and 2500 persons km^{-2} (Ellis 2004), extending this by 1 km to allow for village influence (nearest neighbor analysis 1 km circle), and then by removing all cells with (1) any urban cover, (2) without agriculture or village built-up cover, (3) greater than 75% barren cover, (4) greater than 0% water cover, or (5) population density below 10 persons km^{-2}. Major village regions in Eastern and Central China (VM; Table 1, Figure 1) were mapped within the maximum village extent by eliminating areas in the far West (96° Lon) and North (41° Lat) and patches smaller than 100 km^2 or isolated from larger extents by more than 20 km. Five improved village ''upscaling regions'' (VU; Table 1, Figure 1) analogous to the five initial site and sample selection regions were then mapped within the major village regions based on the regional constraints in supplementary material—Appendix 2. After regions were extracted using GIS, they were edited manually using Landsat Geocover 2000 imagery to identify and eliminate areas without the diagnostic features of village regions (Supplementary material—Appendix 2) or containing large-scale infrastructure atypical of village landscapes (mostly larger built-up areas along roads resulting from town and industrial development).

Table 1. Regions and Sites

	China[1]	Village regions[2]			North China Plain		Yangtze Plain		Sichuan Hilly		Subtropical Hilly		Tropical Hilly	
		Maximum (VP)	Major (VM)	Upscaling (VU)	Region	Gaoyi Site	Region	Yixing Site	Region	Jintang Site	Region	Yiyang Site	Region	Dianbai Site
Extent (10^6 km^2)	9.48	2.56	2.13	0.908	0.276	–	0.086	–	0.084	–	0.284	–	0.178	–
Population (10^6 persons)[3]	1236	847	753	394	165	–	49.3	–	45.3	–	79.2	–	54.8	–
Population density (persons km^{-2})	130	331	354	434	598	726	573	607	539	584	279	495	308	558
Annual precipitation (mm)	1030	1102	1113	1209	670	495	1146	1170	1069	992	1535	1412	1622	1885
Annual mean temperature (°C)	14.3	15.3	15.5	16.7	14.0	13.1	16.0	15.1	17.1	16.5	16.7	17.4	21.0	23.6
Growing days (days)	314	316	315	324	267	260	306	292	363	365	342	329	365	365
Elevation (m)														
Mean	322	285	266	86.7	45.6	52.7	8.2	5.2	386	433	171	77	170	41
Max	5295	3977	3365	824	378	65.0	50	14.0	733	529	824	115	807	241
Slope (%)	17.6	14.4	14.0	9.03	0.83	0.83	0.76	1.1	12.3	11.2	15.2	4.5	14.4	8.3

[1] *Mainland China, excluding Taiwan.*
[2] *Village regions of China (Figure 1): maximum extent (VP), major regions of Eastern China (VM), and the combined extent of all five village regions sampled in this study (VU).*
[3] *Population estimates are for 2000 from Tian and others (2005), precipitation and temperature are based on Willmott and Matsuura (2001), growing days are based on Fischer and others (2000), and elevations and slopes are derived from Space Shuttle Radar Topography Mission 90 m data (National Geospatial-Intelligence Agency 2004).*

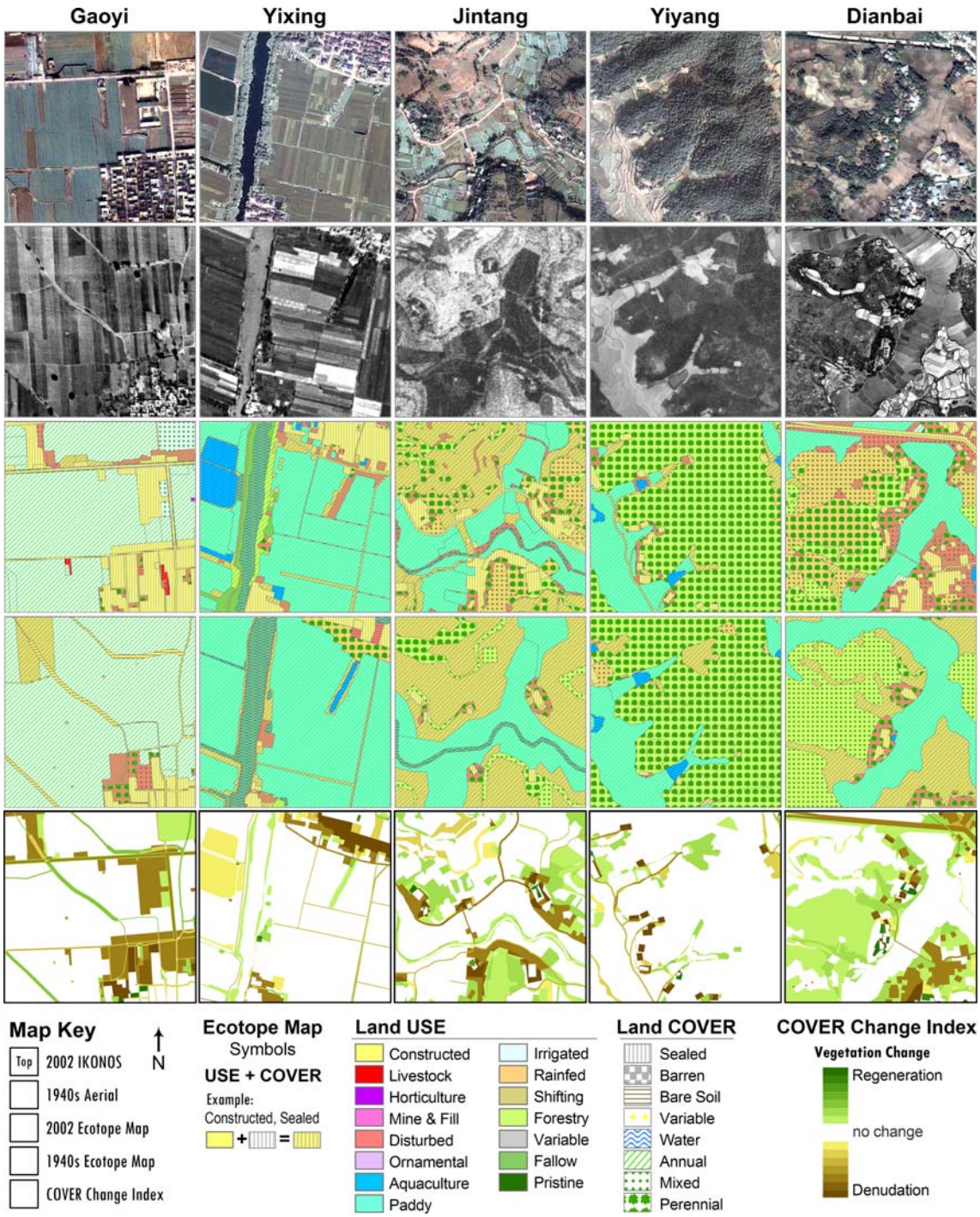

Figure 2. Examples of imagery, ecotope maps, and land-cover changes across a single 500 × 500 m landscape sample cell in each site. Maps follow key at lower left, ecotope maps use ''USE + COVER'' symbols (*bottom center*), and land-cover changes are highlighted using a COVER change index indicating changes in potential for vegetation growth (*lower right*; Ellis and others 2006).

Regional Upscaling

We made regional estimates from sample cell measurements using two different regional upscaling approaches: regional weighting and regional model prediction. In the regional weighting approach, regional estimates (RE) were made by multiplying measurements from each sample cell (CE_i) by ''regional weights'' (RW_i):

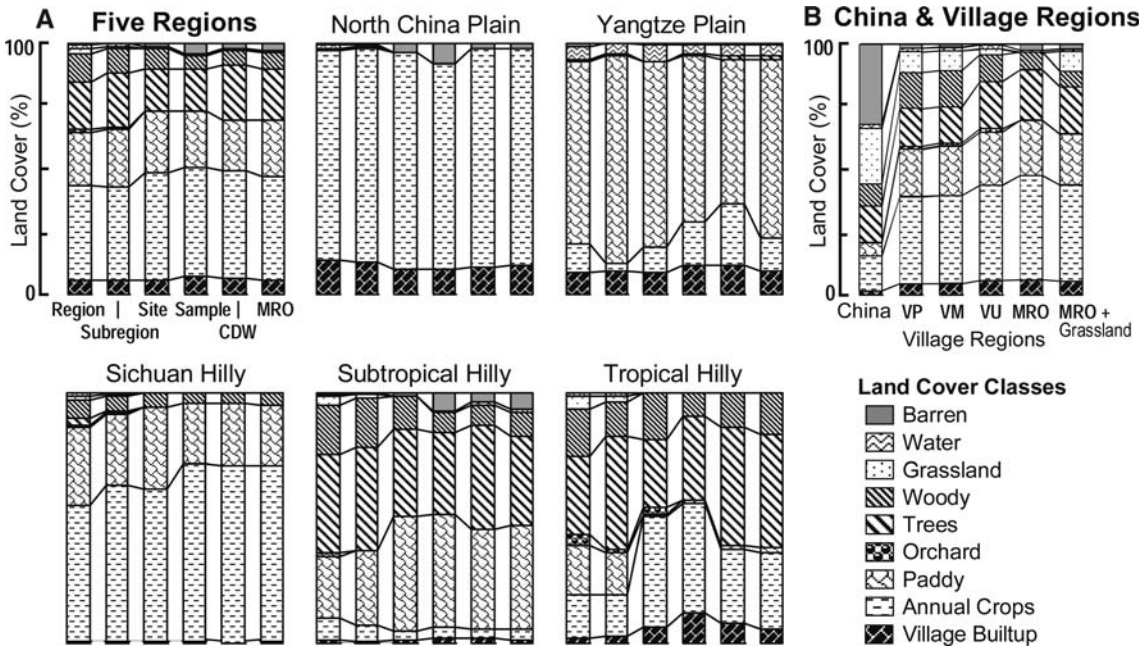

Figure 3. Comparisons of land-cover estimates made from complete regional land-cover data (Liu and others 2003) by different methods. (**A**) Direct estimates within and across five village regions (''Region''), for subregions used for regional stratification of samples (''Subregion''; Figure 1), for sites (''Site''), and for sample cells, both before (''Sample'') and after upscaling by the CDW and MRO procedures. (**B**) Direct estimates for Mainland China compared with the maximum extent of village regions (VP), major village regions in Eastern China (VM), and the combined extent of the five village upscaling regions (VU; Figure 1, Table 1), and MRO upscaled estimates from samples, including correction for Grassland missing from the village upscaling regions. *Note*: ''Region'' and ''MRO'' estimates for ''Five Regions'' in (**A**) are identical with VU and MRO in (**B**), respectively.

$$\mathrm{RE} = \sum_{i}^{n} \mathrm{CE}_i \times \mathrm{RW}_i \qquad (1)$$

Regional ''cluster distance weights'' (CDW) were initially derived from the subregional land-cover cluster data used in sample selection (equation 1 in Ellis 2004). Although this method produced acceptable regional estimates (Figure 3A; Supplementary material—Appendices 3–5; Ellis 2004), we subsequently developed a more powerful regional weighting procedure that made use of complete regional datasets for land cover, population, and terrain. In this procedure, multivariate regional optimization (MRO), weights (w_i) were calculated using an optimization algorithm (Excel Solver; Fylstra and others 1998) that minimized the divergence (D) of sample means (n = 12) from known regional means across a set of J regional variables (X; population density, mean elevation, mean slope, and percent land cover for all classes covering >0.5% of a region and present in the sample; Supplementary material—Appendices 4 and 5):

$$D = \sum_{j=1}^{J} \left| \frac{\bar{X}_j - \sum_{i=1}^{n} \left(x_{j,i} \times w_i \right)}{\bar{X}_j} \right| \times \frac{1}{J} \qquad (2)$$

where $x_{j,i}$ is the value of variable j for sample cell i. D was minimized subject to the constraints that each set of 12 w_is must sum to 1.0 and that w_is may only vary between 0.02 and 0.25, to ensure that all cells participated in the analysis and that no cell completely dominated.

Our second regional upscaling approach, B-spline regional modeling (BRM), was used to predict regional land USE and COVER (Y) from our sampled measurements of these (y) by modeling their relationships with variables measured across regions and also measured for the sample (X; same data as MRO but using only land covers common across regions: village builtup, paddy rice, annual crops, woody cover, tree cover, water, barren). X and y variables were rescaled (Young and others 1976; Young 1981) and then regressed using B-spline expansions (de Boor 1978). Regressions were restricted to regions that had at least one non-zero value of y; Y predictions for regions with all y values equal to 0 were set to 0 (for example, 0% rice paddy in the North China Plain). Supplementary material—Appendices 3–5 and Figure 3 present detailed comparisons between these different types and

scales of regional predictions based on complete regional data.

Change and Uncertainty Analysis

Uncertainties in upscaled regional estimates produced by regional weighting (MRO, CDW) and regional model prediction (BRM) were quantified using different methods. For regional weighting, we combined resampling methods with Monte Carlo observational uncertainty analysis (Ellis and others 2000, 2006). Observational uncertainty models for sampled land class area measurements were parameterized using a feature-based error model and normal probability distribution functions (PDFs; Ellis and Wang 2006). Land class areas were normalized to the total area of each sample cell, including an omission error PDF, and changes in each cell were estimated by subtracting past areas from current areas (a ''zero estimator'' PDF was used for classes missing during one time period or another; Ellis and others 2006). Resampling was conducted at the beginning of each Monte Carlo iteration using a random draw of 12 cells with replacement from the original sample of 12 cells in each site (similar to bootstrapping; Efron and Tibshirani 1991). This was followed by sample weight calculation (MRO, CDW), Monte Carlo draws from PDFs, and finally by the calculations of regionally weighted areas and changes. Frequency distributions from 10,000 Monte Carlo iterations were then used to characterize uncertainties in weighted regional estimates (Supplementary material—Appendices 4 and 5).

Uncertainties in BRM model predictions (Y) were quantified by predicting land USE and land COVER from X across 2500 random samples of 12 grid cells selected at random within 10×10 km ''sites'' distributed at random across each region (= 30,000 values per region; Supplementary material—Appendices 3–5). Change predictions were obtained by subtracting historical from current land USE and COVER predictions after normalizing them to 100% across each cell by dividing them by their sum (Ellis and others 2000). Estimates were then averaged across each 12 cell sample, yielding a random sample of 2500 ''site-based'' regional land-change predictions in each region. Frequency distributions across the 2500 samples were then used to characterize uncertainties in BRM regional change estimates.

We present regional change estimates from both the MRO and BRM upscaling methods, combining the power of optimized regional estimation from sample measurements (MRO) with the conservative regional predictions produced by BRM, which incorporates the full range of regional variation. To quantify our single best estimates of regional change, we average median change estimates by MRO and BRM, and present this together with 90% credible intervals (CI) calculated by averaging the 5 and 95 percentile estimates from MRO and BRM.

Results

Regions, Sites, and Samples

The extent and environmental characteristics of China's village regions are illustrated in Figure 1 and described in Table 1. All together, village landscapes covered approximately 2.5×10^6 km^2 across China, whereas the major village regions of Eastern and Central China occupied 2.1×10^6 km^2, or about 20% of China's total area (Table 1). The major village regions differed substantially and predictably from China as a whole, incorporating more than half of China's total population within an area containing most of China's rice paddy ($>80\%$), annual crops ($>57\%$), and village area ($>71\%$), but with only 21% of its forests, 37% of its shrubland, 9% of its grassland, and less than 2% of its barren areas (Figure 3B). Concentration of population and productive land was even greater within the core area of this study, our five village upscaling regions, which covered 0.91×10^6 km^2 within the major village regions (Table 1; Figures 1 and 3). On average, the village upscaling regions were much warmer, wetter, lower, and flatter than China as a whole, as were the major village regions (Table 1). Still, the village upscaling regions retained major variability in climate, terrain, and land cover, as demonstrated by the substantial environmental differences evident among the five upscaling regions (Table 1 and Figure 3A).

In general, differences among regions were much greater than differences between a region and its representative site (Table 1, Figure 3A). Moreover, differences between site and region were without a clear trend, with the exception of a tendency toward higher population densities and lower mean slopes within sites. More importantly, regional land-cover estimates made by upscaling site-based samples of regional data using MRO, our most powerful regional upscaling procedure, were in good agreement with complete regional data, and this agreement was better than for estimates from entire sites, from unadjusted samples, or for samples upscaled using our original upscaling system (CDW; Figure 3A, Supplementary material—Appendices 4 and 5). Still, there were some significant disagreements

between sampled and direct regional land-cover estimates, especially in the Tropical Hilly Region (missing Paddy) and Subtropical Hilly Region (overabundant Barren land), even after MRO upscaling (Figure 3A, Supplementary material—Appendices 4 and 5). Population density was also significantly overestimated in every region even after MRO upscaling (27% across regions; bias test from Cochran 1977:14; Supplementary material—Appendix 4). Still, MRO upscaling reduced the effect of this and other site-level biases, bringing MRO-upscaled sample estimates into closer agreement with known regional values than did our initial upscaling method, demonstrating the relative effectiveness of this method (Supplementary material—Appendices 4 and 5).

Regional Landforms, Land Uses, and Land Covers

Though population density was fairly constant across regions and sites, regional differences in terrain and climate were associated with major differences in landform (FORM), land use (USE), and land cover (COVER; Table 1, Figures 2–4). Even though a wide diversity of landforms was observed, regions tended to be dominated by a single FORM, mostly by Floodplain in plain regions and by Sloping or Bench Plateau in hilly regions (Figure 4A). Land use and land cover showed similar trends, with the North China Plain dominated by irrigated annual crops, the Yangtze Plain by rice paddy, the Sichuan Hilly Region by rainfed annual crops; the other regions were a mix of crops and Forestry of both open-canopy (Mixed) and closed-canopy (Perennial) trees and woody vegetation (Figure 4B, C). All regions had substantial areas of built structures, ranging from less than 0.5% in the 1940s Tropical Hilly Region to greater than 15% in the 2002 North China Plain, as indicated by Anthropogenic FORM, Constructed, Livestock, and Horticulture USE, and Sealed COVER (Figure 4). Herbaceous (Annual) cover was abundant at all sites due to crop cultivation, whereas extensive patches of woody vegetation and tree cover were present only in hilly areas, where forestry and rainfed orchards were common (Figures 2–4). The characteristic patterns of land forms, uses, and covers within each region were only partially stable between time periods, with most regions showing an increased diversity of these classes at the current time, indicating increasing landscape heterogeneity over time (Figure 4).

Changes in Land Use and Land Cover

Long-term regional changes in land USE and land COVER are presented in Figure 5, using estimates from both the MRO and BRM methods. The most common and well-supported landscape change observed across village regions was a long-term net increase in Sealed land COVER (Figure 5B), a trend paralleled by a widespread increase in Constructed land USE (Figure 5A). Across China's village regions, this change represents a 7% net increase in total regional area covered by impervious built structures (CI = 2–17%), mainly caused by the construction of new buildings and roads. Over the same period, there was a universal decline in herbaceous (Annual) cover, producing an 11% net decrease across regions (CI = −30% to +3%; Figure 5B). In general, declines in herbaceous cover were associated with declines in rainfed crop production, despite an apparent increase in rainfed crops in the Tropical Hilly Region caused by orchard plantings in hilly areas, which displaced forestry there (MRO only; Figure 5A). Another notable change, in which MRO and BRM estimates disagreed, was a large net increase in aquaculture in the Yangtze Plain, associated with the only major landform change observed across regions; the conversion of floodplains to large ponds (Figures 4 and 5).

The most unexpected long-term change observed in this study was a 9% net increase in closed canopy woody vegetation cover across China's village regions (CI = −4% to +21%; Perennial, Figure 5B). Although part of this change is explained by a net increase in new cover by trees and woody vegetation, another part was the result of canopy closure in existing patches of open canopy woody vegetation (Mixed COVER, Figure 5B), causing substantial declines in this COVER in the Hilly Regions.

Landscape Structure and Change at the Ecotope Level

Dominant regional patterns of fine-scale landscape structure are presented in Figure 6, in terms of the 10 most extensive ecotopes in each region and across regions. From this figure, it is clear that a single staple grain crop dominated village landscapes of the Plain and Sichuan Hilly Regions, but not in other regions. The relative complexity of landscapes is also indicated by the degree to which the 10 largest ecotopes accounted for total region area, with shorter columns indicating the fragmentation of landscapes into greater numbers of

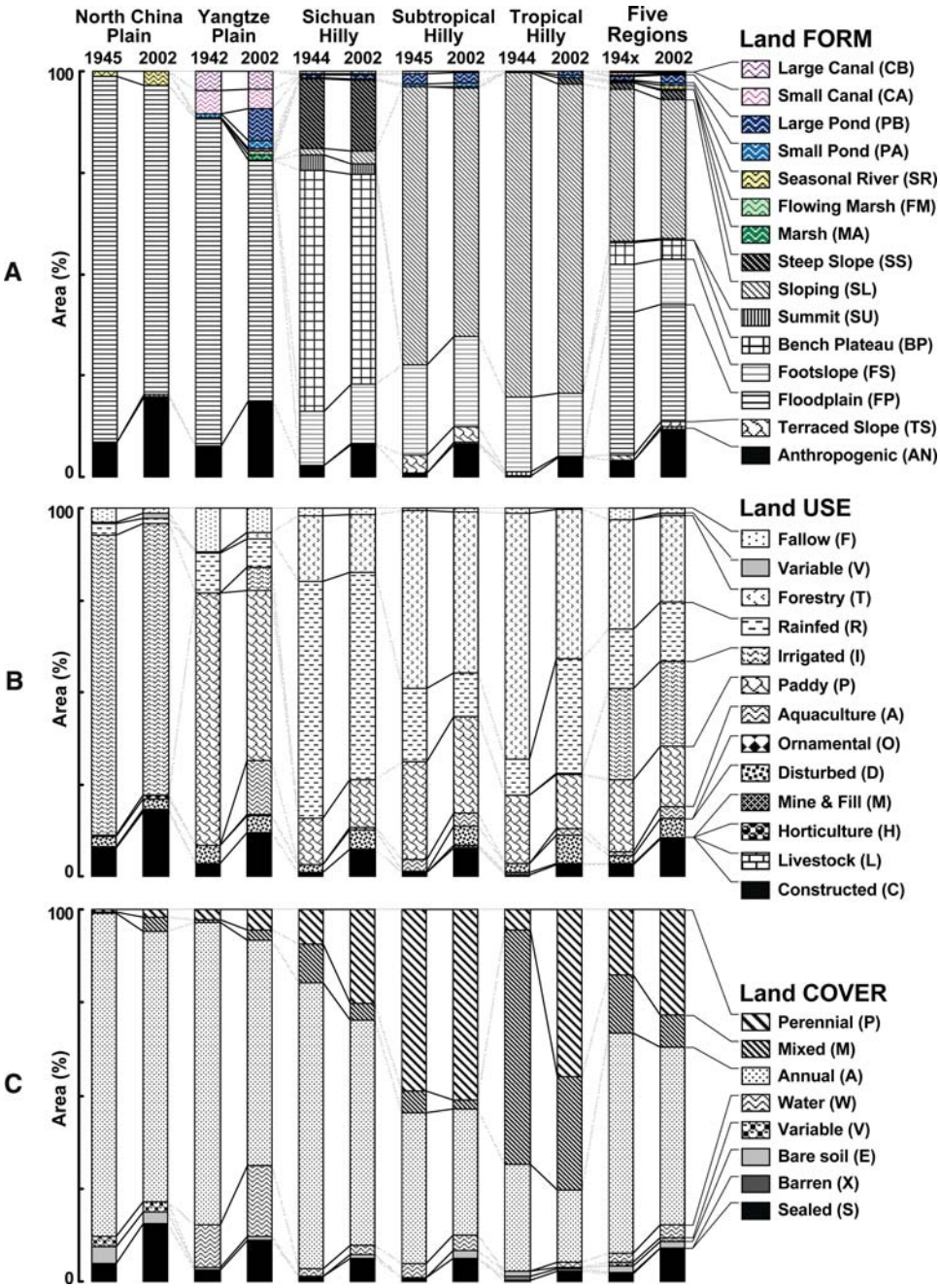

Figure 4. Regional areas of land FORM (**A**), USE (**B**), and COVER (**C**) classes. Areas are MRO-upscaled regional estimates from sample measurements. Only land FORMs covering greater than 1% of a region are shown.

smaller ecotope classes. Based on this interpretation, landscape complexity clearly increased over time in all regions and this is confirmed by long-term increases in the total number of ecotope features and classes, smaller feature areas, and increasing feature perimeters in Table 2. Although this complexity led to fairly large numbers of unique ecotope classes within regions (over 100 in two regions), and especially across all five regions (311 in 2002), most regional area was occupied by a much smaller set of larger ecotope classes (Table 2). More than half of all ecotope classes within any region were small and insignificant in area (<0.25% of a region; Table 2; Ellis and Wang 2006).

Statistics in Table 2 demonstrate that all village regions experienced substantial ecotope-level landscape change and also that some regions experienced far more change than others, with total changed areas ranging from 36% of the North China Plain to 78% in the Tropical Hilly Region. The five largest ecotope area increases and decreases within each region and across regions are described in Figure 7A, together with the 10 largest

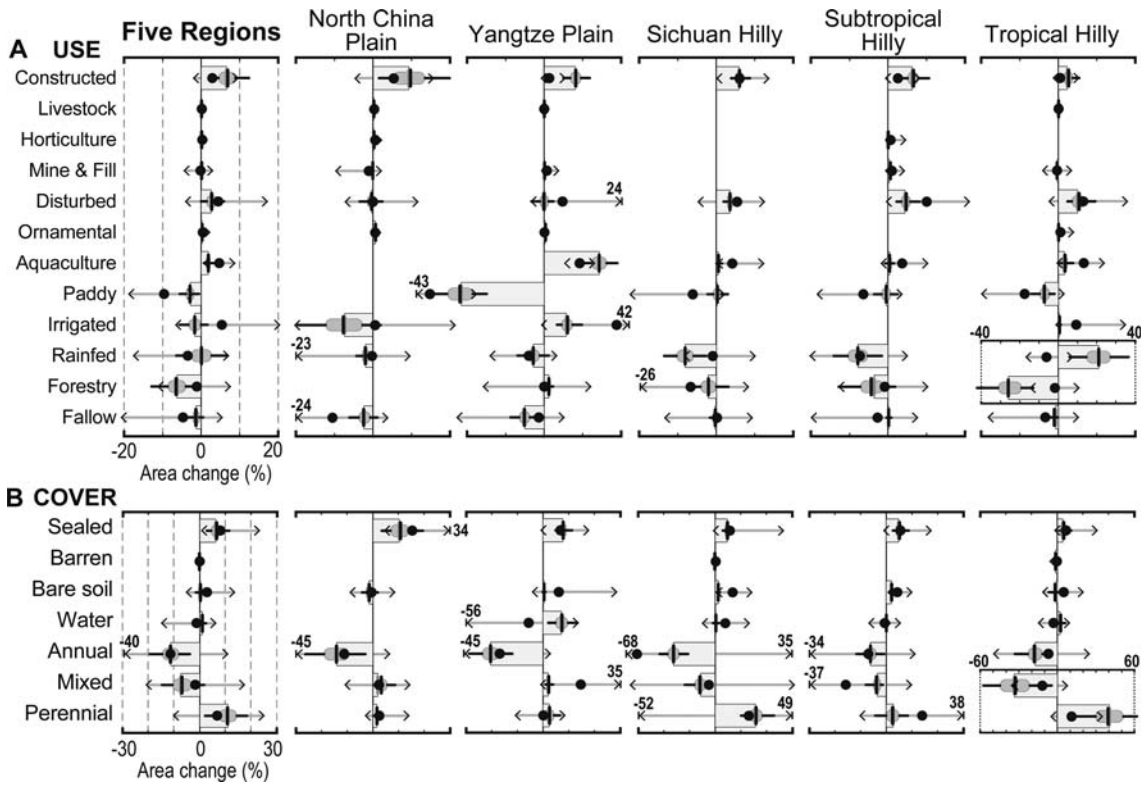

Figure 5. Regional changes in land USE (**A**) and land COVER (**B**) from circa 1945 to 2002. Positive numbers are increases over time. Estimates by both MRO and BRM upscaling methods are provided. MRO median estimates are *wide gray bars*, means are *black vertical lines*, interquartile ranges are *dark gray ovals*, and 90 percentile ranges are *black whiskers*. BRM medians are *black circles*, with a *gray horizontal line* and *angled brackets* enclosing the 90 percentile range. The degree to which the median BRM estimate (*black circle*) falls within the interquartile (*gray oval*) or 90% credible range of an MRO estimate (*black whisker*) is an indicator of confidence in a specific estimate. To the degree that estimates disagree, results may be considered ambiguous and site-level bias is indicated. Classes appearing in only one region are omitted.

ecotope to ecotope transitions (land transformations; Figure 7B). Housing was one of the five largest ecotope area increases in four of five regions and accounted for a major share of the increased built surface area in all regions, accompanied by smaller areas of improved roads (Figure 7A). Figure 7B also shows that the large net decline in herbaceous cropland that is apparent in Figure 5 occurred by a variety of pathways that differed substantially between regions, including housing and road construction in the Plain Regions (for example, irrigated medium-scale staple crops to attached single story houses in the North China Plain), the conversion of rice paddy to aquaculture ponds in the Yangtze Plain, forestry plantings and tree regrowth in the Subtropical Hilly Region (for example, rainfed medium-scale intensive crops to harvested planted conifer forests), and the planting of perennial crops in all regions (orchards, mulberry and nurseries, for example, rainfed small-scale staple crops to rainfed small-scale mandarin orange orchards in the Sichuan Hilly Region, rice paddy to irrigated small-scale mulberry in the Yangtze Plain, and rainfed small-scale staple crops to rainfed large-scale litchi orchards in the Tropical Hilly Region). Similar fine-scale ecotope transformations explained regional gains in closed canopy woody vegetation and tree cover, which occurred mostly by perennial crop plantings in annual crop areas (examples above), by cropland abandonment and woody regrowth (for example, rainfed medium-scale intensive crops to harvested regrowth conifer forest in the Subtropical Hilly Region), and by orchard and forestry plantings and regrowth on relatively denuded hillsides (for example, harvested regrowth open woody vegetation to rainfed large-scale litchi plantings in the Tropical Hilly Region).

In all regions, the diversification of land management and vegetation over time is apparent in ecotope changes and transformations (Figure 7). For example, the largest ecotope decreases in each

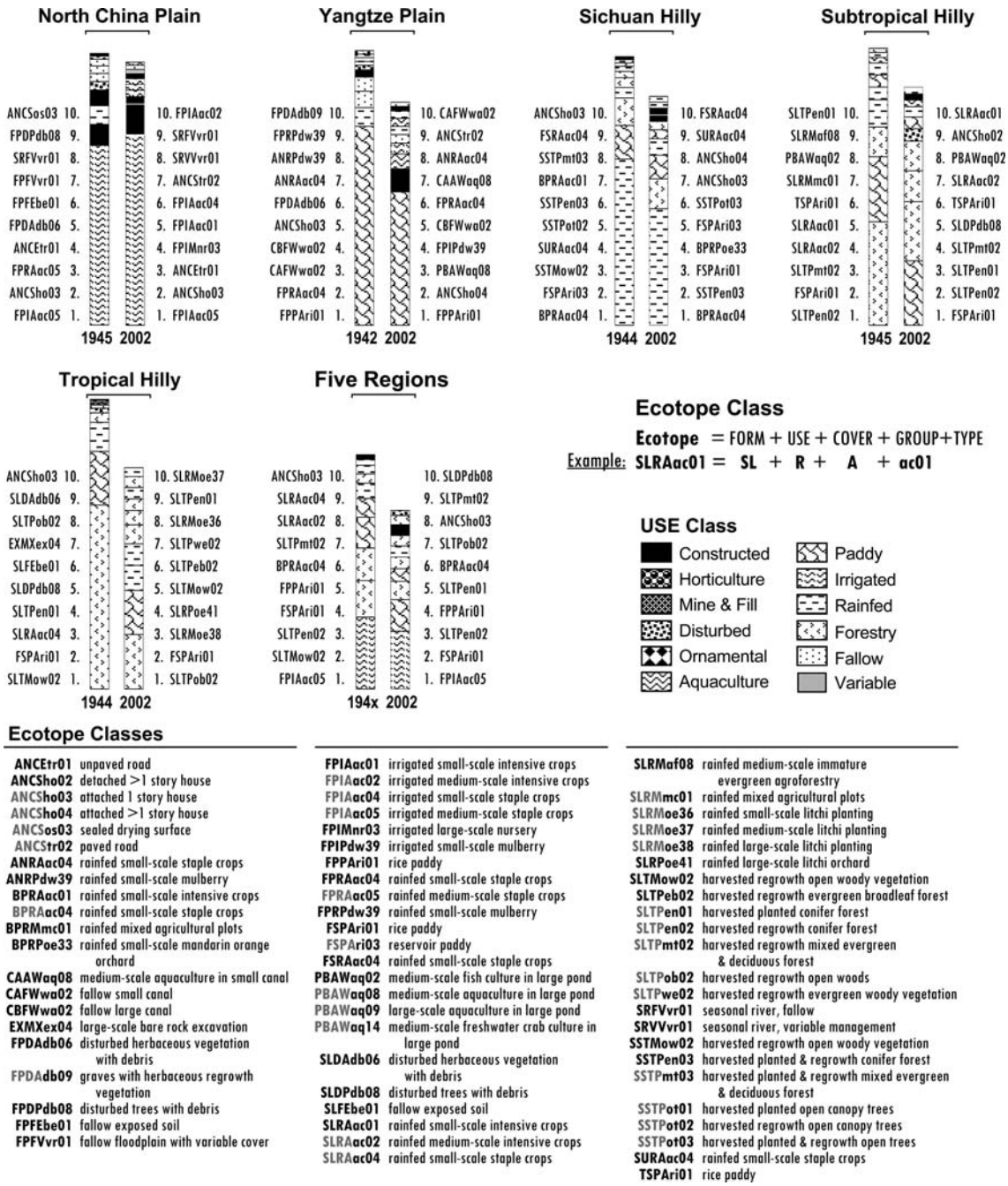

Figure 6. Areas of the 10 largest ecotope classes within and across regions. Ecotopes are sorted by area (largest at bottom), symbolized by USE class (legend) and labeled using standard ecotope classes described at bottom. Ecotope classes are composed from land FORM, USE, and COVER classes (Figure 4) combined with more detailed GROUP + TYPE classes as indicated at the bottom of the figure (details on ecotope classes are online at http://ecotope.org/aem/classification/). Bars are proportional to total regional area, with 100% indicated by a bracket under each site label. Regionally upscaled estimates by MRO.

region were always much larger than the largest increases (Figure 7A) and this usually represented the fragmentation of the largest ecotope classes into a larger number of smaller classes. A good example of this was the fragmentation of harvested woody regrowth patches on hillslopes into five different ecotopes in the Tropical Hilly Region (Figure 7B).

Hundreds of unique ecotope transformation pathways were observed within each region, and the 10 largest ecotope transformations accounted

Table 2. Regional Landscape Patterns, Changes, and Transformations Based on Sample Data

	North China Plain		Yangtze Plain		Sichuan Hilly Region		Subtropical Hilly Region		Tropical Hilly Region		Five regions	
	1940s	2002	1940s	2002	1940s	2002	1940s	2002	1940s	2002	1940s	2002
Population density (persons km^{-2})[1]	485	956	634	994	526	757	235	464	84	355	346	669
Feature count (features km^{-2})	121	257	209	428	168	410	198	342	84	276	151	318
Mean feature area (m^2)	11651	5981	5061	2398	6039	2642	5223	3130	15372	5547	9229	4357
Total perimeter (km km^{-2})	39.1	70.3	66.6	100.7	67.8	105.4	65.1	73.3	34.3	64.4	51.6	76.2
Mean ecotope classes per cell	7.6	15.2	17.6	34.7	13.6	31.7	14.1	22.4	6.0	22.8	10.8	22.3
Ecotope classes (total unique)	28	65	41	110	52	104	31	64	25	82	130	311
Ecotope classes with area >0.25% of region	16	24	15	38	20	31	20	32	10	33	31	58
Area covered by ecotopes with area >0.25% of region	98.5%	97.0%	96.8%	95.9%	97.1%	93.3%	98.5%	98.2%	98.7%	97.2%	94.3%	91.0%
Changed area (%)												
Total	36.1%		50.8%		60.0%		65.1%		78.2%		57.0%	
Ten largest transformations[2]	17.9%		19.8%		26.6%		28.4%		49.3%		14.7%	
Transformations with area >0.25% of region	26.8%		34.9%		40.8%		48.8%		66.6%		28.9%	
Ecotope transformations (number)												
Total	284		772		675		513		381		2517	
Accounting for 90% of change	71		160		153		117		57		419	
Transformations with area >0.25%	31		41		41		49		39		44	

[1] *Population density and other estimates are MRO-adjusted sample cell measurements.*
[2] *Transformations are specific ecotope to specific ecotope transitions.*

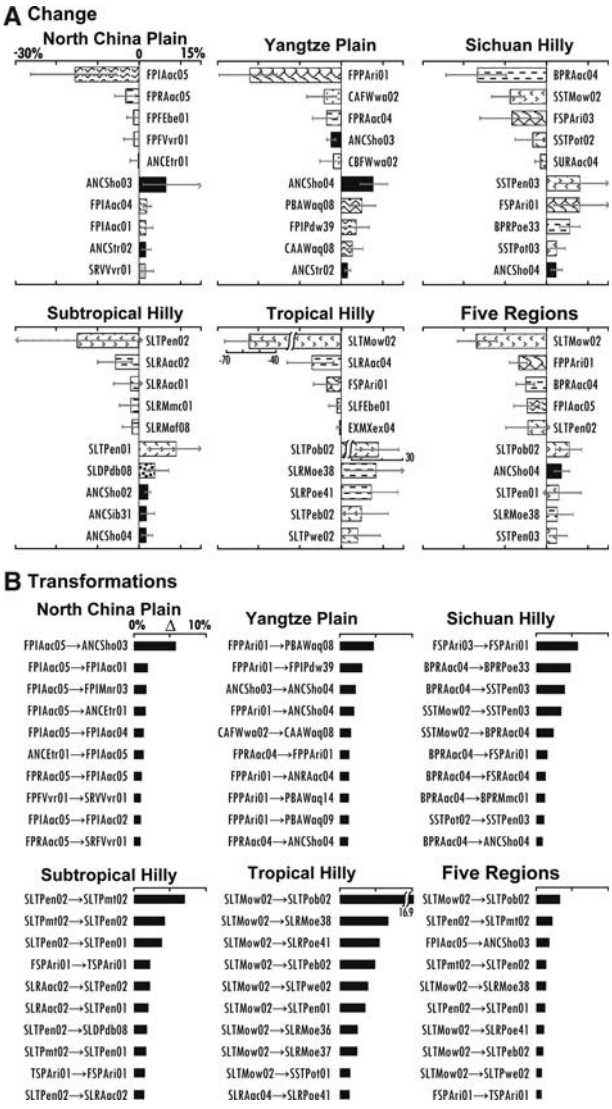

Figure 7. Regional ecotope changes (**A**) and transformations (**B**), circa 1945 to 2002. (**A**) The top five ecotope area decreases (negative; *top*) and top five increases (positive; *below*) within each region and across all five regions are indicated by bars symbolized by USE class, with 90% confidence intervals. (**B**) The top 10 ecotope to ecotope transformations within each region (past → present ecotope transitions) are presented as a percent of region area. Ecotope labels are the same as Figure 6. Regionally upscaled estimates by MRO.

for less than half of all ecotope change, except in the Tropical Hilly Region (Table 2). As a result, a large number of small and poorly measurable ecotope transformations (area < 0.25% of a region; Ellis and Wang 2006; Ellis and others 2006) were required to explain even 90% of changed ecotope area, demonstrating the complexity of ecotope-level change processes and their measurement (Table 2). Simultaneous ecotope transformations in both directions only added to this complexity (for example, the change from cropland to unpaved roads and back again in the North China Plain; Figures 2 and 7B).

Discussion

The Regional and Global Impacts of Fine-Scale Land-Change Processes

Our results confirm that over the past 50 years, China's ancient village landscapes were transformed by major changes in land use and land cover. New buildings, roads, and other anthropogenic structures quadrupled the impervious surface area of village regions, increasing this from 2% in the 1940s to 9% in 2002 (Figures 4 and 5). At the same time, herbaceous vegetation declined by 11%, from 59% in the 1940s to 48% in 2002. And more surprisingly, these changes were accompanied by a 9% net increase in regional cover by closed-canopy woody vegetation, increasing the regional area of this cover from 18% in the 1940s to 28% in 2002 (Figures 4 and 5).

Extending these results across the village regions of Eastern and Central China, an area of more than 2×10^6 km^2, makes it clear that these fine-scale landscape changes are more than capable of globally significant alteration of climate and biogeochemical cycling. For example, a 9% regional increase in closed canopy woody vegetation amounts to approximately 0.2×10^6 km^2 across China's villages (CI = -0.08 to $+0.44 \times 10^6$ km^2), an area equivalent to the total area of China's planted forests in 1998 (Fang and others 2001), or about 3 times the global annual rate of tropical deforestation (Achard and others 2002). Clearly, tree cover changes of this magnitude have the potential to alter regional and even global climate by changing surface albedo, surface heat balance, precipitation and hydrology (Gibbard and others 2005) and indirectly by acting as a sink for atmospheric carbon (Fang and others 2001).

Built surfaces, which tend to have opposite effects on climate, also increased by a total regional area of approximately 0.14×10^6 km^2 (CI = 0.04 to $+0.34 \times 10^6$ km^2), or more than 4 times the total urban area of China in 2000 (0.03×10^6 km^2; Liu and others 2003). This striking result is readily explained by the housing and infrastructure needs of more than 750 million rural people, especially given their increasing wealth and the generally lower density of housing per person in rural areas when compared with urban areas. Although our sampling and upscaling procedures significantly

overestimated regional population density and may therefore have overestimated changes in land use and other parameters related to population density, adjusting for this bias would only lower our regional estimates by about one third (Supplementary material—Appendix 4), reducing the observed village built-up area increase to 3 times, instead of 4 times China's urban area, for example.

Fine-Scale Causes and Consequences of Regional and Global Change

Changes in village land use and land cover might seem to mirror global changes in land cover by extensive landscape-transformation processes, such as urban expansion and forest regrowth (Kauppi and others 2006). Yet, these changes are not equivalent in scale, driving processes, environmental impacts or in the methods required to measure them. Village landscape change is the cumulative result of intensive landscape-transformation processes implemented by hundreds of millions of land managers acting locally at fine spatial scales (Ellis 2004; Ellis and others 2006). As a result, the fine-scale land use transformations that we observed in this study were extremely diverse and complex both within and across village regions (Figure 7, Table 2).

Large regional declines in herbaceous cover (~9% across regions) resulted mostly from the conversion of crop plots to housing, roads, and orchards and by the abandonment of crop plots to woody regrowth. Increased cover by closed canopy woody vegetation was caused by orchard plantings, cropland abandonment, improved forestry practices on sloping land, and by tree planting and regrowth around new houses and roads. Yet even these diverse land-transformation processes are generalizations. The suite of land-transformation processes responsible for even the largest regional changes involved dozens of different transformation pathways that differed substantially between regions (Figure 7, Table 2). Moreover, village landscape structure grew increasingly more heterogeneous and complex over time in all regions, with greater numbers of smaller features divided into an increasing number of ecologically distinct vegetation and land management classes over time (Table 2). Use of high-resolution field-validated ecological mapping allowed for detailed analysis of these land-transformation processes and even for direct interpretation of these in collaboration with their causative agents: local land managers (Wu and others 2009). This should be a fruitful direction for further research, especially when combined with local and regional socioeconomic data and models, offering the potential for even greater understanding of the causes and consequences of intensive landscape-transformation processes in densely populated rural regions (Verburg and Chen 2000).

In global- and even some regional-scale observations and models, the village regions of China are classified as cultivated land mixed with trees and shrubs in hilly areas or as cultivated land mixed with built-up surfaces in the North China Plain and with water in the Yangtze Plain. As a result of this coarse-resolution bias in land-over analysis, China's village landscapes appear largely unchanged in the recent decades for which remotely sensed estimates are available, except for the expansion of built-up and water surface areas in the plain regions, where these changes tend to be clustered and therefore occur in fairly large patches. Although the recent shrinkage of village landscapes by the encroachment of urban areas and towns is readily captured in regional data (Liu and others 2003; Seto and Fragkias 2005), very little reliable regional data exist on long-term landscape changes within village regions and even less on the local causes and environmental consequences of these fine-scale changes, even though villages cover more than 20% of China (Table 1; Ellis 2004). Even widely reported changes in China's forest and agricultural areas (Fang and others 2001; Houghton 2002; Liu and others 2005b) have little relation to long-term changes occurring in villages, because these were almost entirely caused by large-scale deforestation and afforestation projects outside and at the periphery of China's village regions.

Most importantly, the impacts of fine-scale changes in landscape structure on climate and biogeochemistry are poorly understood and may be entirely different from those observed and modeled at coarser scales. At the fine spatial scales at which landscapes vary within village regions, urban heat islands are replaced by dispersed ''rural heat mosaics'' and forests are traded for carefully tended orchards, hedgerows and small stands of one to a few trees. Yet the built structures and woody vegetation of China's villages are at least as extensive as China's urban and afforested lands. Although it is possible that the fine-scale intermingling of these different landscape features moderates their net environmental impacts, there is no strong evidence either for or against this hypothesis at present. And how might these impacts be controlled by local patterns of housing and road construction, cultivation, forestry and land abandonment? Considering the impacts of landscape fragmentation on

habitat suitability and biodiversity (Noss 1990), the ecological consequences of increasing fine-scale landscape heterogeneity in villages clearly merit further investigation, even though these regions have long been densely populated. Fine-scale landscape heterogeneity might appear to be of only local consequence. However, this is the general condition of densely populated anthropogenic landscapes, which already cover a larger portion of Earth's ice-free land than do wild forests (Ellis and Ramankutty 2008).

On Making Regional Change Measurements from Landscape Samples

When designing and interpreting the results of this and other regional studies based on site-based sampling, the methodological limitations of this approach must be considered. First of all, robust statistical procedures must be used to quantify the substantial uncertainties inherent in this technique. Resampling methods proved especially useful for this, as normality, equal variance and independence of variables cannot be assumed. We also observed a trade-off between statistical procedures that emphasize the power of direct observations (for example, MRO), and model-based procedures that incorporate the full range of regional variation but have relatively large uncertainties and weaker linkage with direct observations (for example, BRM; Figure 5). Ideally, these approaches should be combined, with agreements between methods justifying greater confidence in results (for example, Sealed COVER increases in Figure 5). Disagreements between methods, although deflating confidence in regional estimates, should also be examined case by case, with emphasis on the results of direct observations. For example, regional experts confirmed that both aquaculture and water surface area increased substantially in the Yangtze Plain (Wu and others 2009), as predicted by MRO, whereas BRM estimates showed an increase in aquaculture and a decrease in water area, a result both inconsistent and apparently incorrect (Figure 5). Fortunately, both methods generally agreed in estimating land COVER changes, especially when combined across all five regions, although agreement was weaker for land USE estimates, most likely as a result of its greater number of classes.

Regional upscaling of sample data is based on relationships between regional and local variables. Yet these relationships may be weak, or may vary within regions (non-stationarity). Indeed, variation of this type likely caused the high variance in regional estimates by BRM, and may also explain many of the disagreements between estimates by BRM versus MRO. Still, this problem is not unique to site-based methods—it is also a problem for measurements made by complete coverage remote sensing. For example, the spectral properties of rice paddy can vary tremendously within regions because of local differences in irrigation, planting dates, and other factors. As a result, the accuracy of rice paddy classification can vary greatly within regions—an effect readily observed in the China national land-cover dataset. Although variability in relationships between local, fine-scale, land changes and regional variables can be measured, this will require much larger regional samples of historical observations than are ever likely to be available. Fortunately, it is unlikely that spurious regional upscaling relationships could have produced consistent regional change estimates across both of our independent regional upscaling models (MRO versus BRM).

The use of site-based sampling to make regional estimates is also influenced by bias in the selection of sites and samples, such as our limitation to areas covered by 1940s era aerial photography and subregional land-cover data. Although subregional land cover later proved similar to that of entire regions (Figure 3A, Supplementary material—Appendix 4), 1940s aerial photographic coverage clearly favored more populous areas. Even with systematic efforts to avoid field sites with any outward indication of being more densely populated or otherwise anomalous within a region, our sites and samples were significantly biased toward higher population densities than were typical of their regions (Table 1; Supplementary material—Appendix 4). These biases could have been avoided if complete regional data were used for sample selection. Fortunately, we were able to incorporate complete regional data into our regional upscaling procedures at a later stage, thereby reducing both site and sample bias and incorporating the full range of regional variability into uncertainty analyses (Appendices 4 and 5).

Finally, the most fundamental limit to making regional estimates by site-based sampling is its restriction to measuring fine-scale change processes. Urban expansion, large-scale deforestation and other change processes that occur at larger scales than sites are poorly measured by site-based sampling. However, if adequate regional data are available, the degree to which any set of landscape samples captures regional variability can be quantified using regional indicators (Appendices 4 and 5) that can also be used to optimize region, site, and sample configurations toward making specific regional or global estimates in the future.

The Need for Regional and Global Observations of Intensive Land-Change Processes

Regionally stratified landscape sampling revealed a variety of ecologically significant long-term changes across China's village landscapes that would not be observable using conventional methods for land-change measurement (Ellis and others 2006; Ozdogan and Woodcock 2006). Even at 30 m resolution, land-change measurements by remote sensing tend to produce unreliable results in village regions due to their fine-scale landscape heterogeneity (Zhang and others 2000; Zhao and others 2003; Ozdogan and Woodcock 2006). This limitation was evident when comparing China's National land-cover data, which were derived from 30 m resolution Landsat imagery, with observations at field sites. The China national land-cover dataset contained almost no built cover in the Sichuan and Subtropical Hilly regions (Figure 4A versus Figure 5) and misclassified almost all rice paddy in our Tropical Hilly Region site as upland crops (Figure 3A versus Figure 4B). Failure to detect housing in hilly regions makes sense given the fine-scale dispersal of housing and its partial cover by trees and bamboo in these regions, but the missing paddy areas are harder to explain, especially given that many of these were larger than dozens of Landsat pixels. These observations make clear the benefits of sampled landscape estimates over complete coverage remote sensing in densely populated areas, especially in hilly regions with complex terrain.

By enabling the concentration of resource-intensive field measurements within relatively small field sites, regionally stratified site-based sampling provides a generally useful tool for regional and global investigations by ecologists and other field-based researchers, as it greatly reduces logistical costs and thereby facilitates larger sample sizes and more detailed and accurate field measurements than is feasible across large regions using spatially random or systematic sampling. Moreover, the concentration of field research within site-based landscape samples is especially advantageous for investigating the linkages between human activity and long-term ecological change, because at this scale of investigation, interviews with local land managers are readily conducted and can be linked with direct observations on how and why these local actors alter specific ecological patterns and processes (Binford and others 2004; Ellis 2004; Rindfuss and others 2004; Liu and others 2007; Turner and others 2007; Wu and others 2009). In essence, by integrating regional upscaling with site-based sampling, the time-tested interdisciplinary case-study approach to understanding coupled human-natural systems (Rindfuss and others 2004; Liu and others 2007; Turner and others 2007; Wu and others 2009) can be integrated with the regional and global change measurements needed to understand both the causes and the global consequences of local change processes. Finally, resource-efficient measurement strategies are critical if we are to investigate the global and regional impacts of long-term ecological changes within the anthropogenic landscapes that now cover most of Earth's ice-free land (Ellis and Ramankutty 2008), above all because these occur predominantly within the less-well studied agricultural regions of developing nations in Asia, Africa, and Latin America (Ellis and Ramankutty 2008).

Conclusions

China's village landscapes have changed substantially at fine spatial scales since 1945, driving major regional increases in built surfaces and closed canopy tree cover and declines in annual cropped area. Aggregated across China's more than 2 million km^2 of village landscapes, these intensive landscape-transformation processes are likely causing significant regional and global changes in climate, biogeochemistry, and biodiversity that are not anticipated, measured, or explained by conventional coarser resolution approaches to global and regional change measurement and modeling. Given the extent and potential environmental impacts of these changes, further study of intensive land-change processes is merited, especially in the densely populated rural landscapes of developing regions. Where historical data are rare and the costs of fieldwork are large, as they are across most developing regions, regional sampling and upscaling methods offer a critical way forward in investigating the causes and consequences of long-term ecological changes at regional and global scales.

Acknowledgments

This material is based upon work supported by the U.S. National Science Foundation under Grant DEB-0075617 awarded to Erle C. Ellis in 2000. We are very grateful to Xin Ping Liu for research in Hunan, to Shi Ming Luo for supporting research in Guangdong, and to our local collaborators for field assistance across China. Peter Verburg developed our initial regionalization system. Thanks to Kevin

Klingebiel, Kevin Sigwart, Jonathan Dandois, and Dominic Cilento for critical assistance in this project. Thanks to Jiyuan Liu for China land-cover data and to Yongzhong Tian for China population density data. Eric Lecoutre developed R code used in producing supplementary material—Appendix 5. Thanks to Michael Leonard and the National Archives and Records Administration for historical aerial photographs. SpaceImaging provided IKONOS imagery. Erle Ellis thanks Steve Gliessman of the Department of Environmental Studies at the University of California, Santa Cruz, and Chris Field of the Department of Global Ecology, Carnegie Institute of Washington at Stanford for graciously hosting his sabbatical. A final thanks to Greg Asner, Diann Prosser, Mutlu Ozdogan, and our anonymous reviewers for helpful comments on the manuscript. Any opinions, findings, conclusions, or recommendations expressed in this material are those of the authors and do not necessarily reflect the views of the National Science Foundation.

REFERENCES

Achard F, Eva HD, Stibig H-J, Mayaux P, Gallego J, Richards T, Malingreau J-P. 2002. Determination of deforestation rates of the world's humid tropical forests. Science 297:999–1002.

Binford MW, Lee TJ, Townsend RM. 2004. Sampling design for an integrated socioeconomic and ecological survey by using satellite remote sensing and ordination. Proc Natl Acad Sci USA 101:11517–22.

Brewer KRW. 1999. Design-based or prediction-based inference? Stratified random vs stratified balanced sampling. Int Stat Rev 67:35–47.

Cochran WG. 1977. Sampling techniques. New York (NY): Wiley.

de Boor C. 1978. A practical guide to splines. New York: Springer-Verlag.

Efron B, Tibshirani R. 1991. Statistical-data analysis in the Computer-Age. Science 253:390–5.

Ellis EC. 2004. Long-term ecological changes in the densely populated rural landscapes of China. In: DeFries RS, Asner GP, Houghton RA, Eds. Ecosystems and land use change. Washington, DC: American Geophysical Union. p 303–20.

Ellis EC, Li RG, Yang LZ, Cheng X. 2000. Long-term change in village-scale ecosystems in China using landscape and statistical methods. Ecol Appl 10:1057–73.

Ellis EC, Ramankutty N. 2008. Putting people in the map: anthropogenic biomes of the world. Front Ecol Environ 6:439–47.

Ellis EC, Wang H. 2006. Estimating area errors for fine-scale feature-based ecological mapping. Int J Remote Sens 27:4731–49.

Ellis EC, Wang H, Xiao HS, Peng K, Liu XP, Li SC, Ouyang H, Cheng X, Yang LZ. 2006. Measuring long-term ecological changes in densely populated landscapes using current and historical high resolution imagery. Remote Sens Environ 100:457–73.

Fang J, Chen A, Peng C, Zhao S, Ci L. 2001. Changes in forest biomass carbon storage in China between 1949 and 1998. Science 292:2320–2.

Fischer G, van Velthuizen H, Nachtergaele F, Medow S. 2000. Global agro-ecological zones – 2000. FAO Land and Water Digital Media Series Number 11. Food and Agriculture Organization of the United Nations, International Institute for Applied Systems Analysis, Rome.

Foley JA, DeFries R, Asner GP, Barford C, Bonan G, Carpenter SR, Chapin FS, Coe MT, Daily GC, Gibbs HK, Helkowski JH, Holloway T, Howard EA, Kucharik CJ, Monfreda C, Patz JA, Prentice IC, Ramankutty N, Snyder PK. 2005. Global consequences of land use. Science 309:570–4.

Frolking S, Xiao XM, Zhuang YH, Salas W, Li CS. 1999. Agricultural land-use in China: a comparison of area estimates from ground-based census and satellite-borne remote sensing. Global Ecol Biogeogr 8:407–16.

Fylstra D, Lasdon L, Watson J, Waren A. 1998. Design and use of the Microsoft Excel Solver. Interfaces 28:29–55.

Gallego FJ, Delince G, Carfugna E. 1994. Two stage area frame on squared segments for farm surveys. Surv Methodol 20:107–15.

Gibbard S, Caldeira K, Bala G, Phillips TJ, Wickett M. 2005. Climate effects of global land cover change. Geophys Res Lett 32. doi:10.1029/2005GL024550.

Grimm NB, Grove JM, Pickett STA, Redman CL. 2000. Integrated approaches to long-term studies of urban ecological systems. Bioscience 50:571–84.

Han CR. 1989. Recent changes in the rural environment in China. J Appl Ecol 26:803–12.

Heilig GK. 1997. Anthropogenic factors in land-use change in China. Popul Dev Rev 23:139.

Houghton RA. 2002. Temporal patterns of land-use change and carbon storage in China and tropical Asia. Sci China C Life Sci 45:10.

Houghton RA, Hackler JL. 2003. Sources and sinks of carbon from land-use change in China. Global Biogeochem Cycles 17.

Kauppi PE, Ausubel JH, Fang J, Mather AS, Sedjo RA, Waggoner PE. 2006. Returning forests analyzed with the forest identity. Proc Natl Acad Sci USA 103:17574–9.

Liu J, Diamond J. 2005. China's environment in a globalizing world. Nature 435:1179–86.

Liu J, Dietz T, Carpenter SR, Alberti M, Folke C, Moran E, Pell AN, Deadman P, Kratz T, Lubchenco J, Ostrom E, Ouyang Z, Provencher W, Redman CL, Schneider SH, Taylor WW. 2007. Complexity of coupled human and natural systems. Science 317:1513–6.

Liu J, Liu M, Tian H, Zhuang D, Zhang Z, Zhang W, Tang X, Deng X. 2005a. Spatial and temporal patterns of China's cropland during 1990–2000: an analysis based on Landsat TM data. Remote Sens Environ 98:442.

Liu J, Tian H, Liu M, Zhuang D, Melillo JM, Zhang Z. 2005b. China's changing landscape during the 1990s: large-scale land transformations estimated with satellite data. Geophys Res Lett 32:1–5.

Liu JY, Liu ML, Zhuang DF, Zhang ZX, Deng XZ. 2003. Study on spatial pattern of land-use change in China during 1995–2000. Sci China D Earth Sci 46:373–384.

National Geospatial-Intelligence Agency, 2004. Shuttle Radar Topography Mission DTED Level 1 (3 arcsecond). National Center for Earth Resources Observation and Science (EROS).

Noss RF. 1990. Indicators for monitoring biodiversity: a hierarchical approach. Conserv Biol 4:355–64.

Ozdogan M, Woodcock CE. 2006. Resolution dependent errors in remote sensing of cultivated areas. Remote Sens Environ 103:203.

Rindfuss RR, Walsh SJ, Turner BL II, Fox J, Mishra V. 2004. Developing a science of land change: challenges and methodological issues. Proc Natl Acad Sci USA 101:13976–81.

Schreuder HT, Gregoire TG, Weyer JP. 2001. For what applications can probability and non-probability sampling be used? Environ Monit Assess 66:281.

Seto KC, Fragkias M. 2005. Quantifying spatiotemporal patterns of urban land-use change in four cities of China with time series landscape metrics. Landscape Ecol 20:871.

Tian Y, Yue T, Zhu L, Clinton N. 2005. Modeling population density using land cover data. Ecol Model 189:72–88.

Turner BL II, Lambin EF, Reenberg A. 2007. The emergence of land change science for global environmental change and sustainability. Proc Natl Acad Sci USA 104:20666–71.

Verburg PH, Chen Y. 2000. Multiscale characterization of land-use patterns in China. Ecosystems 3:369–85.

Vitousek PM, Mooney HA, Lubchenco J, Melillo JM. 1997. Human domination of Earth's ecosystems. Science 277:494–9.

Wang H, Ellis EC. 2005. Spatial accuracy of orthorectified IKONOS imagery and historical aerial photographs across five sites in China. Int J Remote Sens 26:1893–911.

Willmott CJ, Matsuura K. 2001. Terrestrial air temperature and precipitation: monthly and annual climatologies (Version 3.02). Center for Climatic Research, Department of Geography, University of Delaware.

Wu J-X, Cheng X, Xiao H-S, Wang H, Yang L-Z, Ellis EC. 2009. Agricultural landscape change in China's Yangtze Delta, 1942 to 2002: a case study. Agric Ecosyst Environ 129:523–33.

Wulder MA, Hall RJ, Coops NC, Franklin SE. 2004. High spatial resolution remotely sensed data for ecosystem characterization. Bioscience 54:511.

Young F. 1981. Quantitative analysis of qualitative data. Psychometrika 46:357–88.

Young F, de Leeuw J, Takane Y. 1976. Regression with qualitative and quantitative variables: an alternating least squares method with optimal scaling features. Psychometrika 41:505–29.

Zhang JY, Dong WJ, Wu LY, Wei JF, Chen PY, Lee DK. 2005. Impact of land use changes on surface warming in China. Adv Atmos Sci 22:343–8.

Zhang W, Zhuang D, Hu W. 2000. Area summarization in establishing the national resources and environmental database. J Remote Sens (Beijing) 4:304–10.

Zhao J, Sun Y, Bai G, Wu G, Shao G. 2003. Certainties and uncertainties of land cover statistics in China. J Environ Sci (China) 15:520–4.

Online Supplement

Appendix 1. Initial Regionalization, Site Selection, Sampling and Imagery

Initial regionalization and site selection. China's village regions were initially identified as densely populated (>150 persons km^{-2}) agricultural areas (>5% cultivated land; Ellis 2004) and then stratified into five environmentally distinct initial regions for site selection (Figure 2A) using a *K*-means cluster analysis of 32 km gridded data on terrain, climate, and soil fertility (Verburg and others 1999; Ellis 2004). A single 100 km^2 rectangular field research site was then selected within each initial region (Figure 2D; sites were 7 × 14.25 km, except Gaoyi site = 9 × 11.1 km). Sites were selected in areas with adequate historical aerial photographic coverage, greater than 10 km distance away from any major city, and with no evidence of regionally anomalous environmental or socioeconomic conditions, including exceptionally high or low soil fertility, wealth, development level, major water bodies, industry or mines, as assessed using regional maps and other data after the field reconnaissance of at least three potential sites per region together with regional experts (Ellis 2004).

Regional sample selection within sites. To maximize the regional-representativeness of the small area that we were able to map within each 100 km^2 site, we distributed this among twelve 500 m square grid cells selected using a regionally stratified balanced sampling design (Ellis 2004). First, we imposed a 500 m square sampling frame across China, thereby obtaining landscape sample units practical both for high-resolution mapping and local fieldwork and for the integration of these with regional and global remote sensing (Townshend and Justice 1988; Gallego and others 1994; Ellis 2004; Ellis and others 2006). Next, land cover across a "sampling subregion" within each initial region (two adjacent Landsat scenes, except for the Yangtze Plain) was obtained by supervised classification of Landsat ETM+ Geocover 2000 imagery, the highest quality spatially explicit regional data obtainable at the time of sampling (Figure 2C; 8 land cover classes, overall accuracy >84%, κ >0.81; Ellis 2004). The subregion's grid cells were then stratified into 3 to 4 major land-cover clusters using *K*-means cluster analysis of grid cell land-cover proportions (Ellis 2004). Finally, a regionally stratified balanced sample of $n = 12$ grid cells was selected within each site by selecting three or more replicate grid cells from each land-cover cluster based on its subregional abundance, with priority given to cells with the lowest Euclidean distance from cluster means (Ellis 2004). Only cells with complete coverage by both IKONOS and historical imagery were selected, and selection was biased toward non-adjacent replicate cells for each cluster (Ellis 2004). This procedure yielded regionally balanced site-based samples (Figure 2D) with Landsat land-cover proportions more similar to those for entire subregions than those for entire sites (Ellis 2004).

Site imagery. Following site selection, IKONOS 4 band pan-sharpened 1 m resolution GEO imagery was acquired across each site (Figure 2E; winter 2001/2002 except Yixing: summer 2002) and orthorectified from ground control points obtained by submeter accuracy Global Positioning Systems (GPS) and digital elevation models (Wang and Ellis 2005). Historical aerial photographs for China, circa 1945, were obtained from the U.S. National Archives and Records Administration (NARA; RG-373, www.archives.gov) and orthorectified using tie points from orthorectified IKONOS imagery (Wang and Ellis 2005).

Sample mapping. The 12 grid cells sampled within each site were mapped using anthropogenic ecotope mapping (AEM; Ellis and others 2006), a scale-explicit high-resolution ecological mapping procedure designed to recognize all ecologically distinct features (ecotopes) with dimensions of 2 m or more in both current and historical high resolution imagery (≤ 1 m). Ecotope features were mapped by a

single trained interpreter at each site using a Geographic Information System (GIS), first by direct interpretation of land use and vegetation cover polygons in orthorectified imagery, and then by repeated validation, correction, and classification of all ecotope features in the field, assisted by current (2002) and historical (1940s) local land managers (Ellis and Wang 2006; Ellis and others 2006). AEM classification accuracy was greater than 85% ($\kappa > 0.85$) across sites and time periods (Ellis and Wang 2006), and is based on a four level *a priori* classification hierarchy, FORM→ USE→ COVER→ GROUP+TYPE, combining basic landform, land-use and land-cover classes (FORM, USE, COVER) with a set of more detailed feature management and vegetation classes (GROUPs) stratified into TYPEs (Ellis and others 2006; http://ecotope.org/aem/classification). Whereas each level of feature classification, including land USE and land COVER, is independent, allowing for separate analysis at each level, full ecotope classification integrates the four classification levels within each feature. For example, a forest of closed canopy regrowth evergreen trees (GROUP+TYPE = en02) on a gentle slope (FORM = SL = Sloping) managed for harvest (USE = T = Forestry) with Perennial COVER (P; >60% woody cover) is classified as the ecotope "SLTPen02" (FORM+USE+COVER+GROUP+TYPE).

Population density within sampled cells was estimated by enumerating houses in imagery and determining each household's population assisted by village accountants (2002) and elders (1940s). Maps of landscape changes and estimates of land transformations were made by intersecting current and historical maps using GIS and analyzing ecotope to ecotope transitions ("ecotope transformations") in the "change features" thus created.

References Cited

Ellis EC. 2004. Long-term ecological changes in the densely populated rural landscapes of China. In: DeFries RS, Asner GP, Houghton RA, Eds. Ecosystems and land use change. Washington, DC: American Geophysical Union. p 303–20.

Ellis EC, Wang H. 2006. Estimating area errors for fine-scale feature-based ecological mapping. Int J Remote Sens 27:4731–49.

Ellis EC, Wang H, Xiao HS, Peng K, Liu XP, Li SC, Ouyang H, Cheng X, Yang LZ. 2006. Measuring long-term ecological changes in densely populated landscapes using current and historical high resolution imagery. Remote Sens Environ 100:457–73.Townshend JRG, Justice CO. 1988. Selecting the spatial resolution of satellite sensors required for global monitoring of land transformations. Int J Remote Sens 9:187–236.

Verburg PH, Veldkamp A, Fresco LO. 1999. Simulation of changes in the spatial pattern of land use in China. Appl Geogr 19:211–33.

Wang H, Ellis EC. 2005. Spatial accuracy of orthorectified IKONOS imagery and historical aerial photographs across five sites in China. Int J Remote Sens 26:1893–911.

Appendix 2. Constraints and Diagnostic Features Used in Delineating Village Regions

	North China Plain	Yangtze Plain	Sichuan Hilly Region	Subtropical Hilly Region	Tropical Hilly Region
Constraints					
Mean slope (%)	≤2.5	≤2.5	>2.5	>2.5	-
Elevation (m)	-	<50	<550	<550	<550
Patch sizes (km^2)	>100	>10	>25	>100	>25
Other constraints	Within the North China Plain; no rice paddy	South of the Huai River; within 2 km of rice paddy (to compensate for paddy underestimation in the CNLCD)	Within the Sichuan Basin	North of initial Tropical Hilly Region; annual precipitation <1200 mm*	South of initial Subtropical Hilly Region, no plains >10 km^2; >5 km from cities; >2 km from coastlines
Diagnostic features					
Terrain	Alluvial plains	Alluvial plains laced with canals	Narrow "brain-like" terraced hills and valleys	Mountain fringes & narrow hills with narrow, canal-free floodplains	Hills to low mountains interspersed with small plains
Vegetation & agriculture	Irrigated annual crops, no paddy.	Paddy-dominated, some mulberry & orchards.	Paddy in valleys, crops & trees on hills	Paddy in plains & low terraces, hills with trees & shrubs (incl. tea; annual crops rare)	Hills with trees, shrubs & orchards & without annual crops; paddy in plains & small terraces
Housing	Very large villages (up to 1 km^2).	Small and medium villages, usually along canals.	Dispersed along hill edges: no large villages	Dispersed along hill edges: no large villages	Villages in plains; dispersed housing in hills

* based on 0.1 degree interpolation of Willmot and Matsuura (2001).

Appendix 3. Scales and Types of Regional Estimates

Code	Scale	Description
A0	Region	Initial village region (one of five).
A1	Region	Improved village upscaling region (one of five; set of all 500 m × 500 m grid cells, Appendix 4).
A2	Region	Random sample of 12 grid cells across a single upscaling region (A1).
A3	Region	Random sample of 12 grid cells selected within randomly located 10 km × 10 km sites within a single upscaling region (A1).
A4	Subregion	Subset of initial village region (A0) covered by Landsat Geocover 2000 imagery used to generate data for sample selection within sites (set of grid cells, Appendix 4).
A5	Site	100 km^2 site (all grid cells).
A6	Sample	Sample of 12 grid cells selected within a site.
A7	Sample > Region	Region estimate from 12 cell sample by CDW method.
A8	Sample > Region	Region estimate from 12 cell sample by MRO method.
A9	Sample > Region	Region estimate from 12 cell sample by BRM method.

Appendix 4. Data on Regions, Sites, Samples and Effectiveness of Regional Upscaling

Region	North China Plain	Yangtze Plain	Sichuan Hilly	Subtropical Hilly	Tropical Hilly
Site	Gaoyi	Yixing	Jintang	Yiyang	Dianbai
Province	Hebei	Jiangsu	Sichuan	Hunan	Guangdong
Site center (Longitude, Latitude)	114.600, 37.642	119.577, 31.392	104.748, 30.567	112.475, 28.354	111.332, 21.643
Upscaling Region (A1) Weight[a]	30.4%	9.4%	9.3%	31.3%	19.6%
Initial Region (A0) Weight	28.2%	8.1%	17.6%	33.5%	12.6%
Cells in region (A1[b])	1,079,416	333,934	334,887	1,112,944	688,081
Cells in sampling subregion (A4)	155,832	68,369	73,497	136,359	99,169
Cells in site (A5)	329	314	354	329	332
Significant land-cover classes not in sample[c]	Water (1.1%)	-	Grassland (1.2%), Trees (3.0%)	Grassland (3.6%), Orchard (0.9%)	Grassland (4.9%), Water (1.5%)
Population bias ratio[d]					
Unadjusted sample (A6)	0.131	0.063	0.069	0.493	0.615
MRO-adjusted sample (A8)	0.222	0.086	0.054	0.377	0.319
Divergence (*D*) from the regional mean[e]					
Random cells (A1)	0.47	0.70	0.58	0.78	0.88
Random samples (A2)	0.36	0.59	0.28	0.28	0.30
Random site-based samples (A3)	0.38	0.60	0.45	0.55	0.63
Sampling subregion (A4)	0.10	0.37	0.16	0.20	0.22
Site (A5)	0.52	0.25	0.19	0.54	0.75
Unadjusted sample (A6)	1.30	0.41	0.30	0.62	1.20
CDW-adjusted sample (A7)	0.39	0.49	0.31	0.53	0.80
MRO-adjusted sample (A8)	0.29	0.28	0.24	0.45	0.64
Regional Representativeness (*E*) relative to random (A2) / random site-based (A3) sampling within each region[f]					
Sampling subregion (A4)	1.0 / 1.0	0.96 / 0.97	0.94 / 1.0	0.84 / 1.0	0.84 / 1.0
Site (A5)	0.18 / 0.20	1.0 / 1.0	0.86 / 1.0	0.03 / 0.53	0.0 / 0.29
Sample (A6)	0.02 / 0.04	0.91 / 0.93	0.42 / 0.91	0.01 / 0.34	0.0 / 0.05
CDW-adjusted sample (A7)	0.40 / 0.47	0.77 / 0.80	0.40 / 0.90	0.03 / 0.55	0.0 / 0.24
MRO-adjusted sample (A8)	0.74 / 0.81	0.99 / 1.0	0.67 / 0.97	0.08 / 0.76	0.01 / 0.47

[a] Region weights = region area / total area of five regions.

[b] Codes in parentheses are described in Appendix 3.

[c] Modified CNLCD land-cover classes covering greater than 0.5% of a region but not present within sample.
[d] Difference between estimated and correct regional population density divided by the estimate.
[e] D calculated by equation 2; smaller values indicate greater similarity to the regional mean. A1 and A2 are the median of 10,000 samples, A3 is from 2500 samples, others are direct estimates.
[f] $E =$ 1 – percentile(D) in samples by methods A2 and A3. Values near 1 are optimal for the sampling method.

Appendix 5. Regional Variation in Population, Terrain and Land Cover Across Regions Compared with Regional Estimates from Unadjusted and Upscaled Samples

Frequency distributions for entire regions (A1, Appendix 3), estimates of the regional mean from random sampling (A2), site-based random samples (A3), resampling of original samples (A6), CDW-upscaled samples (A7) and MRO-upscaled samples (A8). All data are normalized to the correct regional mean for each variable, with perfect agreement indicated by a triangle at 1.0 on each x axis (x axes are scaled identically, y axes are scaled to maximum frequency). Plots incorporate a small black diamond at the mean, a horizontal line at the median, shaded interquartile range, and whiskers drawn to the 5th and 95th percentiles (95 percentiles >3.0 are enumerated directly). Only land-cover classes covering greater than 0.5% of a region and present within sample are shown, Appendix 4. Data for A2 is from 10,000 random samples, A3 from 2500 random samples, and data for A6, A7 and A8 represent 10,000 MC iterations with resampling.

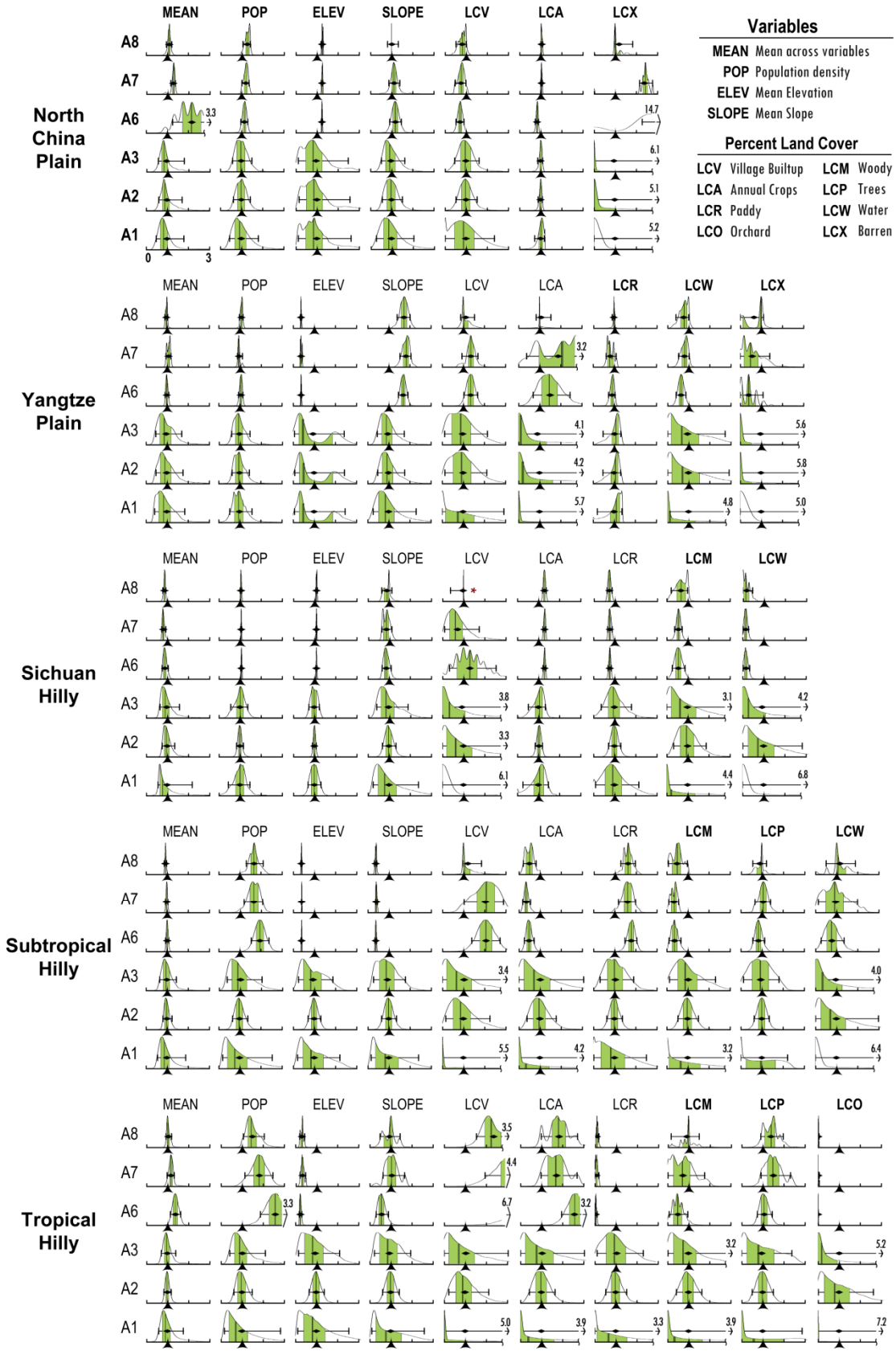
North China Plain
Yangtze Plain
Sichuan Hilly
Subtropical Hilly
Tropical Hilly
MEAN
POP
ELEV
SLOPE
LCV
LCA
LCR
LCM
LCP
LCW
LCO
LCX
A8
A7
A6
A3
A2
A1
Variables
MEAN Mean across variables
POP Population density
ELEV Mean Elevation
SLOPE Mean Slope
Percent Land Cover
LCV Village Builtup
LCA Annual Crops
LCR Paddy
LCO Orchard
LCM Woody
LCP Trees
LCW Water
LCX Barren